Available online at www.sciencedirect.com
SCIENCE DIRECT®
Journal of Nuclear Materials 327 (2004) 19–26
journal of nuclear materials
www.elsevier.com/locate/jnucmat

Estimation of stress corrosion cracking sensitivity of type 304 stainless steel by magnetic force microscope

Shigeru Takaya [a,*], Takayuki Suzuki [b], Yoshihiro Matsumoto [c], Kazuyuki Demachi [a], Mitsuru Uesaka [a]

[a] *Nuclear Engineering Research Laboratory, School of Engineering, The University of Tokyo, 2-22 Shirakata Shirane, Tokai-mura, Naka-gun, Ibaraki-ken 319-1188, Japan*
[b] *Advanced Materials and Structural Integrity Group, Institute of Mechanical Systems Engineering, National Institute of Advanced Industrial Science and Technology, 1-2-1 Namiki, Tsukuba-shi, Ibaraki-ken 305-8564, Japan*
[c] *Nuclear Fuel Industries Ltd., 950 Noda, Kumadori-cho, Sennan-gun, Osaka-fu 590-0481, Japan*

Received 20 January 2003; accepted 8 January 2004

Abstract

An application of a magnetic force microscope (MFM) to the measurement of the chromium depleted regions of type 304 stainless steel is proposed to enable more effective evaluation of the material sensitization to stress corrosion cracking than the conventional methods. The MFM images of sensitized materials show that the magnetizations are induced along grain boundaries by the chromium depletion. The dependence of the magnetization on the sensitization condition conforms to the expected one from the behavior of chromium depletion. Furthermore, the phase identification was performed by electron backscattered pattern technique to reveal the magnetization mechanism due to sensitization. Then, it was found that the magnetization is caused by the transformation from austenite phase to martensite phase. From the discussion on the temperature at which martensitic transformation starts, we see that it seems to be possible to detect regions where the chromium concentration is under 14% by using an MFM.

PACS: 81.70

1. Introduction

Type 304 stainless steel (304SS) is used widely as a structural material in nuclear fission power plants because of its good workability and corrosion resistance. However, heat treatments during welding make it sensitive to stress corrosion cracking (SCC) in corrosive environments. Sensitization is associated with the chromium depletion near grain boundaries caused by the precipitation of chromium carbides at grain boundaries. Particularly, the extent of chromium depletion at a grain boundary is a direct indication of the material's susceptibility to SCC [1]. Other factors such as chromium depletion width and carbide spacing contribute less significantly to SCC susceptibility. In addition to the extent of chromium depletion at a grain boundary, however, the distribution of grain boundary chromium concentrations also becomes very important when one seeks to determine whether or not a continuous SCC crack can initiate, propagate, and continue from one grain boundary to the next through a sensitized material. Hence, development of methods for the quantitative measurement of the distribution of chromium depletion along grain boundaries with high spatial resolution and easy operations is very important for the prediction and prevention of SCC. Until now, several methods have

* Corresponding author. Address: Japan Nuclear Cycle Development Institute, 4002 Narita-cho, O-arai-machi, Ibaraki-ken 311-1393, Japan. Tel.: +81-29 267 4141; fax: +81-29 267 7148.
E-mail address: takaya.shigeru@jnc.go.jp (S. Takaya).

0022-3115/$ - see front matter © 2004 Elsevier B.V. All rights reserved.
doi:10.1016/j.jnucmat.2004.01.016

been developed. For example, the oxalic acid etch test is used as a preliminary screening test. This test can be performed easily, but the evaluation is qualitative [2]. Analysis of grain boundary chemistry with a transmission electron microscope and an energy dispersive X-ray spectrometer can provide precise chromium depletion profiles across grain boundaries, but it has a big problem that the observation area is so narrow [1]. On the other hand, an electrochemical potentiokinetic reactivation test is quantitative and nondestructive, but this test provides only the average value taken over many grain boundaries and gives little information about each grain boundary [3].

We have paid attention to magnetic property as a candidate of an estimation parameter of material sensitization because magnetic property is one of the most sensitive physical properties to degradation such as dislocation and plastic deformation [4]. We have proposed a magnetic method for the sensitization estimation by using a magnetic force microscope (MFM). Concerning with Inconel 600 alloy, the possibility of the quantitative estimation by this method has been shown [5]. In this study, this method is applied to 304SS and the magnetic microstructures of sensitized 304SSs are presented. Furthermore, the phase identification is performed by electron back-scatter pattern (EBSP) technique in order to see if there are any differences of crystal structures between a solution-annealed sample and a sensitized one. This observation results will lead the reason why the magnetic property changes due to sensitization. Finally, the possibility of sensitization estimation by using an MFM is discussed.

2. Experimental procedures

2.1. Material

The plates of 304SS (40 mm × 60 mm × 1.27 mm) were used in this study. Their chemical compositions are listed in Table 1. Each plate (SS-1, 2, 3, 4 or 5) was solution-annealed at 1120 °C for 30 min, followed by a water quench and then subjected to an isothermal heat treatment at 620 °C for various periods as shown in Table 2.

2.2. Etch test

Ten percentage oxalic acid etch test is one of the easy and simple methods for the sensitization estimation of austenitic stainless steels [2]. Each sample was polished mechanically and then etched for 90 s with the electric density of 1 A/cm^2. After the etch test, the etched surfaces were observed by a scanning electric microscope (SEM).

Table 2
Conditions of the heat treatments

Sample number	Heat treatment
SS-1	Solution-annealed
SS-2	Solution-annealed + 620 °C/6 h
SS-3	Solution-annealed + 620 °C/9 h
SS-4	Solution-annealed + 620 °C/18 h
SS-5	Solution-annealed + 620 °C/43 h

2.3. MFM observation

A commercial MFM (SII SPI3700), which employs the phase modulation method, was used throughout this study. In this system, phase shifts ($\Delta\theta$) between the oscillation of the cantilever and the piezoelectric actuator are measured. For small amplitude of the cantilever, this phase shift can be written as follows:

$$\Delta\theta = \frac{Q}{k}F', \tag{1}$$

where Q is the free-oscillation quality factor ($\approx 165 \pm 10$ in the air), k is the spring constant (≈ 3 N/m) and F' is the vertical gradient of the magnetic force on the tip of the cantilever. F' can be expressed by

$$F'(\mathbf{r}) = \frac{\partial F}{\partial z} = \int_{\text{tip}} \frac{\partial^2}{\partial z^2}\{\mathbf{M}^{\text{tip}}(\mathbf{r}') \cdot \mathbf{H}^{\text{sample}}(\mathbf{r}+\mathbf{r}')\}\,\mathrm{d}V', \tag{2}$$

where $\mathbf{M}^{\text{tip}}(\mathbf{r}')$ is the magnetization of the volume element in the tip and $\mathbf{H}^{\text{sample}}(\mathbf{r}+\mathbf{r}')$ is the stray field from the sample [6].

The liftoff between the tip and the sample surface is about 100 nm. Specimens were polished mechanically and magnetized perpendicularly to the plane by the external magnetic field (~0.4 T) before the MFM observation.

2.4. Observation of phase distributions

The distribution of the austenite phase and the martensite phase were observed about the solution-annealed sample (SS-1) and the most severely sensitized

Table 1
Chemical composition of 304SS

Element	Fe	Ni	Cr	C	Si	Mn	P	S
Wt%	71.89	8.65	18.12	0.05	0.43	0.83	0.027	0.002

sample (SS-5) by EBSP technique. EBSP technique can present crystallographic and phase information on bulk samples in a SEM with a spatial resolution of sub-micron order [7]. When an electron beam is focused on a tilted specimen, 70° in our observations, electrons are diffracted with the crystal planes according to the Bragg condition and create a pattern composed of arranged Kikuchi bands on the detector. This pattern is termed an EBSP. The geometrical arrangement of these bands is a function of the phase and the orientation of the crystal lattice within the diffracting volume. In this study, the crystal phases and orientations were determined automatically from EBSPs according to a ranking factor based on the number of votes [8] and the fit parameter by utilizing the software of TexSEM Laboratories Inc.. The votes give the most probable solution out of all possible solutions, and the fit parameter is defined by the average angular deviation between the recalculated bands and the detected bands.

Specimens were polished mechanically at first and then polished electrolytically to remove the plastic deformation layer induced by mechanical polishing.

3. Results and discussions

3.1. Etch test

The SEM images after the etch test are presented in Fig. 1(a)–(e). The etched surface of SS-1 is classified as step structure. It means that there is no chromium depletion in the solution-annealed state. On the other hand, small ditches can be recognized along grain boundaries on the etched surface of SS-2. The ditch shows roughly where chromium is depleted. The ditches become more continuous and the number of ditched grain boundaries increases with heat treatment time. In the case of SS-5, almost grain boundaries seem to have been ditched.

3.2. MFM observation

Fig. 2 shows the surface topography and the MFM image at the same observation region of SS-5. The scanning area is 50×50 μm^2. It should be noted that specimens for MFM observations were polished mechanically but were not etched electrolytically. Although we cannot recognize the grain boundaries in the topography, the MFM image shows them clearly. Small magnetic domains are formed continuously along grain boundaries. On the other hand, the MFM image of the solution-annealed sample does not show any significant magnetization distribution. Therefore, we can see that the magnetization in Fig. 2 is induced by sensitization.

MFM images of SS-2, 3, 4 and 5 are presented in Fig. 3(a)–(d). The scanning area is 50×50 μm^2. The magnetized parts along grain boundaries can be recognized in all the images. They become more continuous and the number of magnetized grain boundaries increases with heat treatment period. This tendency is the same with that of ditches observed by the etch test.

The average total length of magnetized parts along grain boundaries per one scanning area is plotted in Fig. 4. The error bars in the figure show standard deviations. The total length of the magnetized parts along grain boundaries increases monotonously. This result also agrees well with the expected one from the behavior of the chromium depletion in the etch test. These results show that MFM observation can present the morphology of sensitized grain boundaries.

As mentioned before, it is suggested that the major indication of the material's susceptibility to SCC is the extent of chromium depletion at a grain boundary. The average amplitude of MFM signals per one scanning area, which has the possibility of having some relations to the extent of chromium depletion, is plotted in Fig. 5. The error bars in the figure show standard deviations. The average amplitude of MFM signals per one scanning area increases until around 25 h and after that it saturates or decreases slightly. It was reported that the chromium depleted content at a grain boundary increases until several tens hours with heat treatment time and then decreases gradually due to the redistribution of chromium [9,10]. The agreement between the time variation of the range of MFM signals and that of chromium depleted content shows the possibility of quantitative evaluation of the chromium depleted content at grain boundaries, although additional examinations are needed.

From these results, we can see that the quantitative measurement of the distribution of chromium depletion along grain boundaries with high spatial resolution and easy operations is possible by using an MFM.

3.3. Observation of phase distributions

At first, the distribution of the austenite phase of the solution-annealed sample (SS-1) is presented in Fig. 6. The measurement pitch is 0.25 μm. The colors represent crystal orientations according to a color coded unit triangle of the inverse pole figure. The black spots are where the phase decisions were impossible. It often appears on a grain boundary because an EBSP at such a place is superposition of EBSPs from two or more different oriented crystals. In Fig. 6, three grains can be recognized and all parts of them are formed of the austenite phase. At other observation regions also, all of grains were formed of the austenite phase and the martensite phase could not be observed. It is well known that the austenite phase is paramagnetic and the

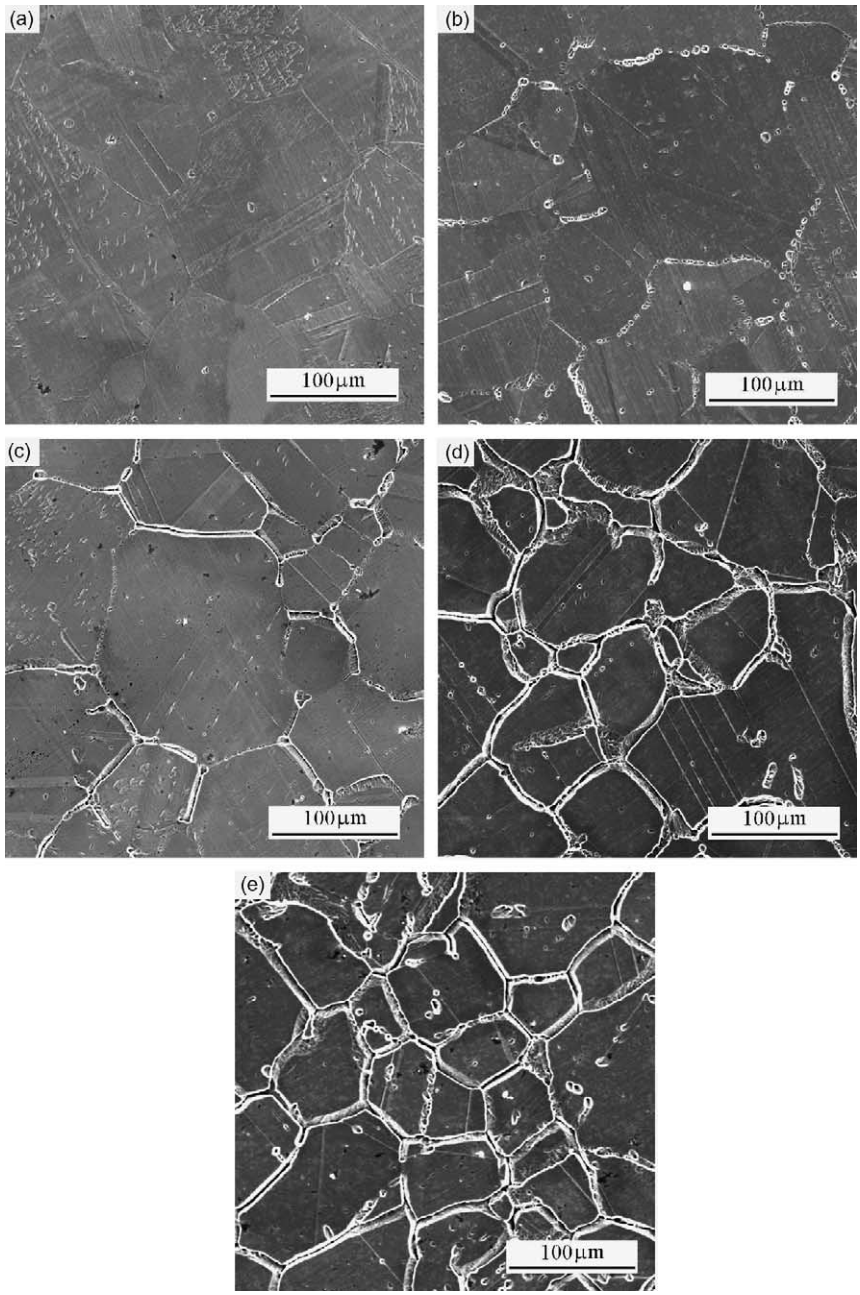

Fig. 1. SEM images after the etch test: (a) SS-1 (only solution annealing), (b) SS-2 (solution-annealing + 620 °C/6 h), (c) SS-3 (solution-annealing + 620 °C/9 h), (d) SS-4 (solution-annealing + 620 °C/18 h), SS-5 (solution-annealing + 620 °C/43 h). The etch surface of SS-1 has step structure. Therefore, it is confirmed that there is no chromium depletion in the solution-annealed state. On the other hand, the ditches along grain boundaries can be recognized on the surfaces of sensitized samples. It shows that the chromium is depleted near grain boundaries. The ditches become more continuous and the number of ditched grain boundaries increases with heat treatment time.

martensite phase is ferromagnetic. This result coincides with the fact that magnetization region could not be observed in solution-annealed state by the MFM.

The distributions of the austenite phase and the martensite phase of SS-5 are shown in Fig. 7(a) and (b), respectively. The measurement pitch is 0.25 μm. Most

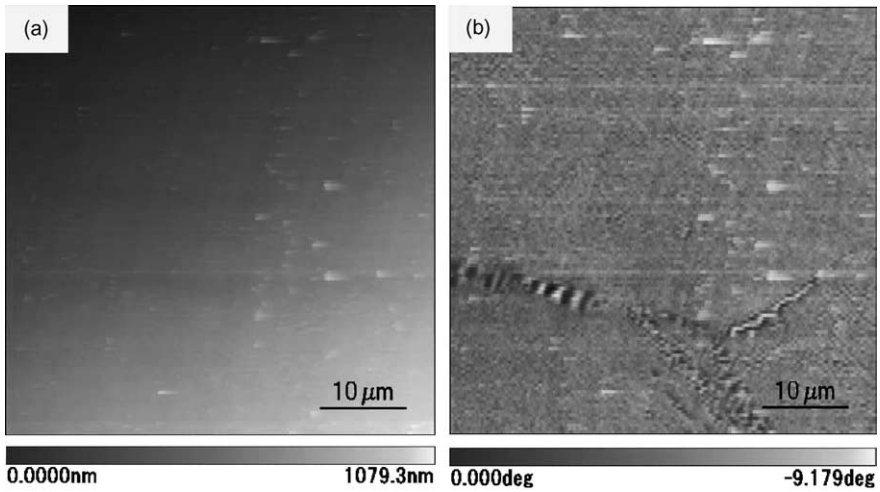

Fig. 2. Images of SS-5 (solution-annealed + 620 °C/43 h). The tip-sample distance is 100 nm. The scanning area is 50×50 μm^2. (a) Topography observed by the atomic force microscope does not show the grain boundaries. (b) The MFM image shows the magnetization distribution near the grain boundaries. The phase shift range is about 9.18°.

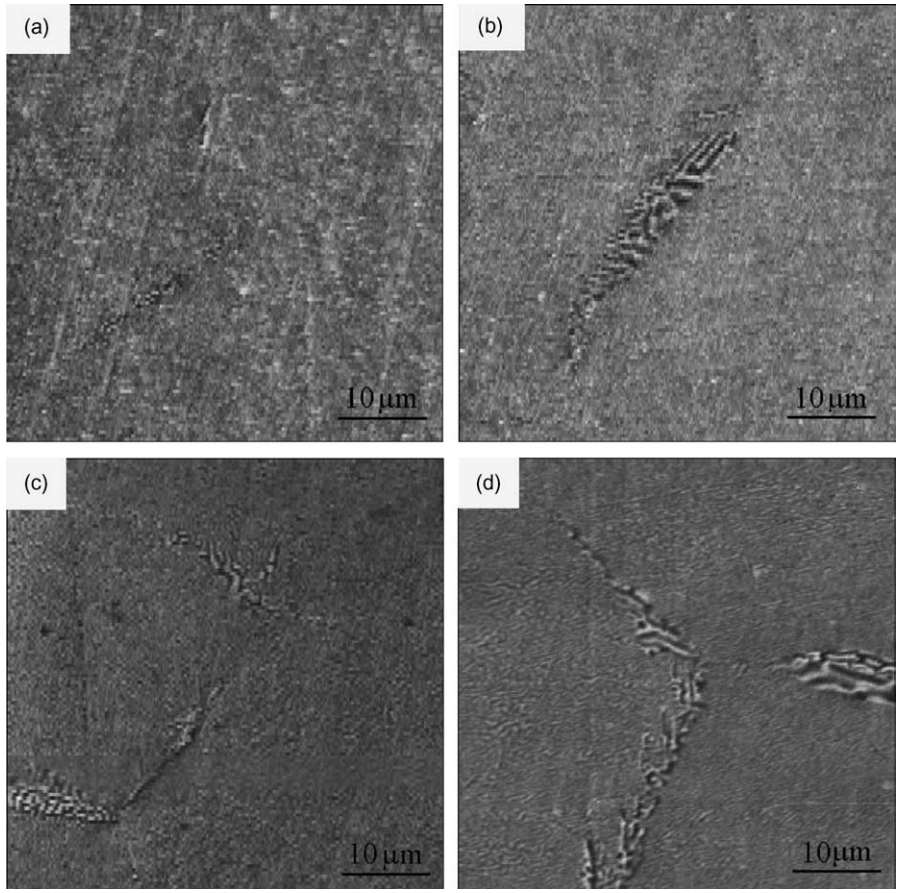

Fig. 3. MFM images of sensitized 304SSs. The tip-sample distance is 100 nm. The scanning area is 50×50 μm^2. (a) SS-2 (solution-annealed + 620C°/6 h); (b) SS-3 (solution-annealed + 620C°/9 h); (c) SS-4 (solution-annealed + 620C°/18 h); (d) SS-5 (solution-annealed + 620C°/43 h). The phase shift ranges are about 3.9°, 4.6°, 7.9° and 8.7°, respectively.

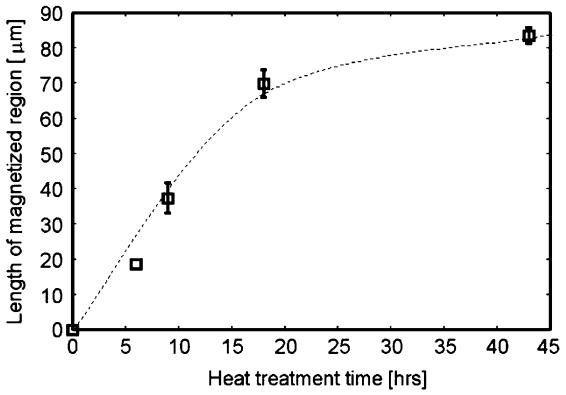

Fig. 4. Time dependence of the average total length of the magnetized regions along grain boundaries per one scanning area.

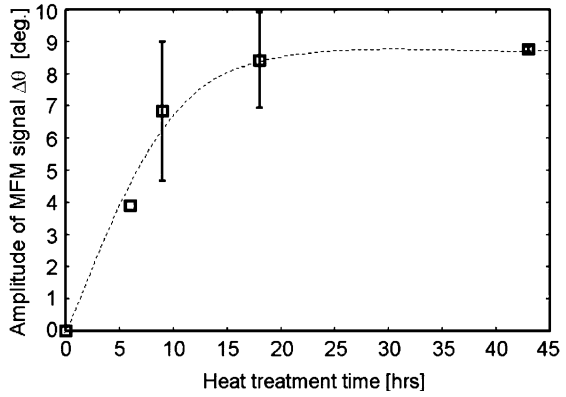

Fig. 5. Time dependence of the average amplitude of MFM signals per one scanning area.

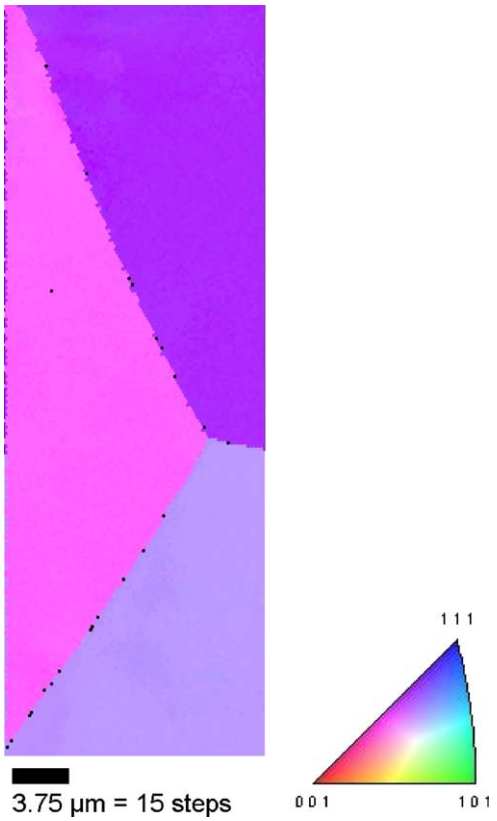

Fig. 6. Distribution of the austenite phase in the solution-annealed sample (SS-1). The measurement pitch is 0.25 μm. The color in the figure represents the crystal orientation according to a color coded unit triangle of the inverse pole figure. About SS-1, the martensite phase was not recognized anywhere.

parts of grains are formed of the austenite phase like SS-1 in the solution-annealed state, but it can be recognized that the martensite phase appears locally along some of grain boundaries. The samples of EBSP from the austenite and martensite phases are presented in Figs. 8 and 9, respectively. The EBSPs are clear enough for the phase analysis and agree well with the recalculated bands in both cases, so the phase differentiations were achieved correctly. Since the martensite phase could not be observed in solution-annealed state, we can say that this phase is induced by sensitization. As mentioned before, the martensite phase shows ferromagnetism, so there is the possibility that the magnetization along grain boundaries observed in sensitized samples by the MFM is the martensite phase. In fact, comparing the morphologies of the magnetization and the martensite phase shown in Figs. 3 and 7, respectively, those are very similar to each other. Next, the average maximum widths over 10 grain boundaries are compared. The average width of the martensite phase is 2.28 ± 1.37 μm and that of magnetization observed in SS-5 by the MFM is 3.94 ± 1.88 μm. The average widths are also similar. The reason why the width of magnetization is a little bit larger than that of the martensite phase will be that the MFM observation area was larger than that of phase observation. Therefore, we can conclude that the magnetization observed by MFM is the martensite phase induced along grain boundaries.

In the case of 304SS, the temperature at which the phase transformation from the austenite phase to the martensite phase starts, Ms point, is given by the following equation [11]:

$$\mathrm{Ms}(^{\circ}\mathrm{C}) = 502 - 810[\%\mathrm{C}] - 1230[\%\mathrm{N}] - 13[\%\mathrm{Mn}] - 30[\%\mathrm{Ni}] - 12[\%\mathrm{Cr}] - 54[\%\mathrm{Cu}] - 46[\%\mathrm{Mo}]. \quad (3)$$

The Ms point of the sample used in this study is estimated about −26.2 °C. It shows that the matrix is formed of the austenite phase in solution-annealed state

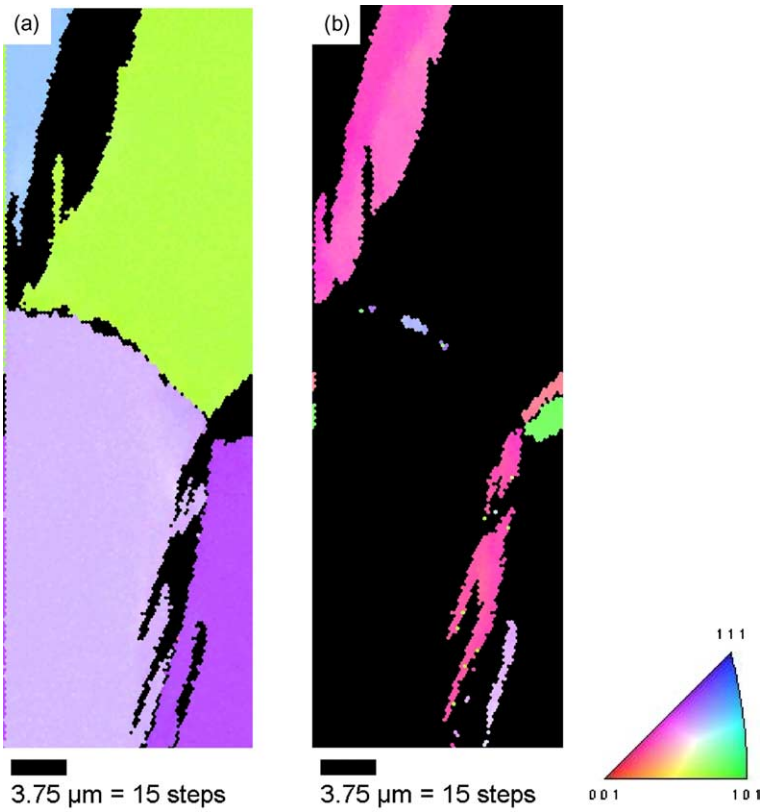

Fig. 7. Images of the phase distributions in the sensitized sample (SS-5): (a) the austenite phase, (b) the martensite phase. The martenite phase, which was not detected in SS-1, is formed locally along grain boundaries.

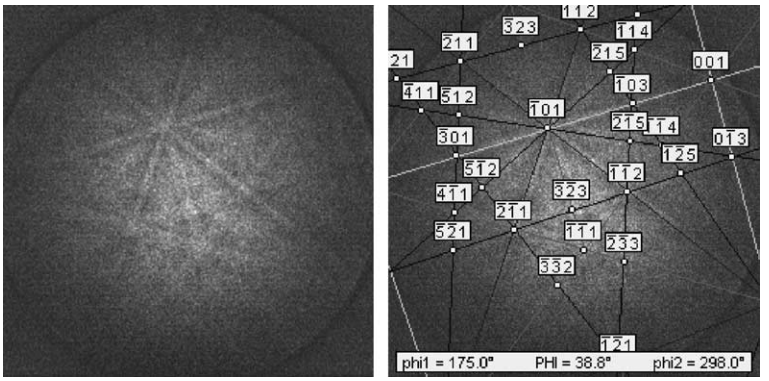

Fig. 8. EBSP from the austenite phase without and with recalculated bands.

at the room temperature. This estimation agrees with our results. However, the chromium is generally depleted near grain boundaries when the austenitic stainless steels are subjected to heat treatments from 500 to 800 °C. In the sensitized state, the Ms point become above the room temperature where the content of chromium decreases by about 4% or more, and the martensite phase will appear.

From this discussion, it seems to be possible to detect a region where the chromium concentration is under 14% by MFM observation. This detection limit is acceptable because it is reported that the susceptibility to SCC increases dramatically when the chromium concentration is under about 13% [1].

It was shown that EBSP technique is also able to be one of the estimation methods of sensitization.

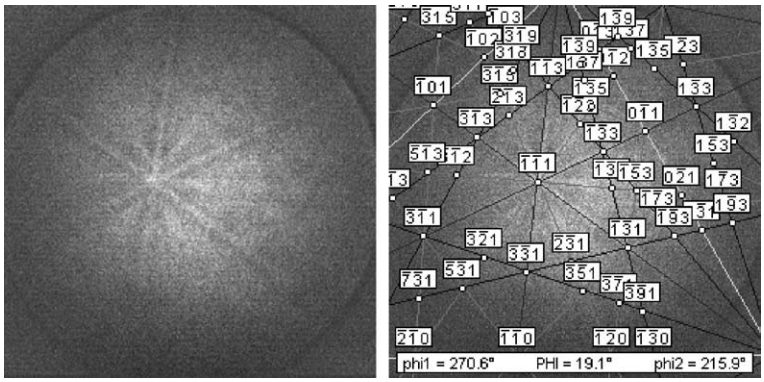

Fig. 9. EBSP from the martensite phase without and with recalculated bands.

However, this technique requires vacuum environment and electropolishing of samples. In addition, the spatial resolution of EBSP technique is about five times lower than that of MFMs.

4. Conclusion

We have proposed the application of an MFM to the measurement of the distribution of chromium depletion along grain boundaries. In this study, this method is applied to 304SS. MFM images of 304SSs sensitized in various conditions showed the magnetized regions along grain boundaries corresponding to the chromium depleted regions observed by the etch test. Time dependences of the amplitude of MFM signals and the total length of magnetized regions along grain boundaries per one scanning area conformed to the expected ones from the behavior of chromium depletion. From these results, we see that it is possible to evaluate the extent of chromium depletion at grain boundaries, which is a major factor to induce SCC, and observe the distribution of grain boundary chromium concentrations at the same time by using MFMs. In addition, it is also an advantage to the conventional methods that MFM observations can be performed with minimal sample preparation and relatively easy operations.

Moreover, the phase identification of 304SSs was performed by using EBSP technique. It was found that though all the observation regions were formed of the austenite phase in the solution-annealed state, the martensite phase existed along grain boundaries in the sensitized state. The morphologies and the average maximum widths of the martensite phase and the magnetization observed by the MFM are similar to each other. This fact shows that the magnetization due to sensitization is caused by the phase transformation from the austenite phase to the martensite phase. It follows from the discussion on the Ms point that MFMs seem to enable to detect region where the chromium concentration is under 14%. This detection limit is acceptable because it is reported that the susceptibility to SCC increases dramatically when the chromium concentration is under about 13%.

Acknowledgements

The Authors would like to thank to Professor K. Miya, International Institute of Universality, and Professor N. Sekimura, the University of Tokyo, for useful suggestions and Dr Y. Nagae, Japan Nuclear Cycle Development Institute, for fruitful discussions.

References

[1] S.M. Bruemmer, B.W. Arey, L.A. Charlot, Corrosion 48 (1992) 42.
[2] Japanese Industrial Standards Committee, JIS G 0571, 1980, in Japanese.
[3] M.A. Gaudett, J.R. Scully, J. Electrochem. Soc. 140 (1993) 3425.
[4] M. Uesaka, A. Gilanyi, T. Sukegawa, K. Miya, K. Yamada, S. Toyooka, N. Kasai, A. Chiba, S. Takahashi, K. Morishita, K. Ara, N. Ebine, Y. Isobe, in: R. Albanese, G. Rubinacci, T. Takagi, S.S. Udpa (Eds.), Electromagnetic Nondestructive Evaluation (II), IOS, Amsterdam, 1998, p. 39.
[5] S. Takaya, T. Suzuki, T. Uchimoto, K. Miya, J. Appl. Phys. 91 (2002) 7011.
[6] D. Ruger, H.J. Mamin, P. Guethner, S.E. Lambert, J.E. Stern, I. McFadyen, T. Yogi, J. Appl. Phys. 68 (1990) 1169.
[7] N. Cheneau-Spath, R.Y. Fillit, J.H. Driver, J. Appl. Crystallogr. 27 (1994) 980.
[8] S.I. Wright, B.L. Adams, Metall. Trans. A 23 (1992) 759.
[9] M. Osawa, F. Ikezu, Boshoku Gijutsu 34 (1985) 331 (in Japanese).
[10] S.M. Bruemmer, L.A. Charlot, Scr. Metall. 20 (1986) 1019.
[11] F.B. Pickering, Appl. Sci. Publ. (1976) 229.